Air intake modelling with fuzzy AFR control of a turbocharged diesel engine

Amir H. Shamdani*, Amir H. Shamekhi and M. Ziabasharhagh

Department of Mechanical Engineering,
K.N. Toosi University of Technology,
Tehran, Iran
E-mail: a.h.shamdani@gmail.com
E-mail: shamekhi@kntu.ac.ir   E-mail: mzia@kntu.ac.ir
*Corresponding author

Abstract: One of the most vital factors in combustion control is Air-to-Fuel Ratio (AFR) estimation and control. In this work a detailed mathematical, nonlinear and control oriented model of dynamic processes of turbocharged diesel engines is presented. This model has been developed using physical equations and also experimental data. Common Rail Injection (CRI) that is a flexible fuel injection system in which quantity, timing and pressure of injection are controllable separately is chosen for this purpose. AFR control is performed making use of fuzzy logic methodology with a fast fuzzy controller. All above-mentioned models are programmed in Matlab/Simulink software.

Keywords: AFR control; CRI; common rail injection; computer simulation; fuzzy logic methodology; intake system; VGT; variable geometry turbocharger.

Biographical notes: Amir Hossein Shamdani has received his MSc in Mechanical Engineering from K.N. Toosi University of Technology. His research interests include internal combustion engines, automotive control systems and engine modelling and simulation.

Amir Hossein Shamekhi has received his PhD in Mechanical Engineering from K.N. Toosi University of Technology. He is an Assistant Professor in Mechanical Engineering Department. His research interests are in the areas of internal combustion engine control systems and engine modelling and simulation. He is the author of many research studies published in various journals and conference proceedings.

Masoud Ziabasharhagh has received his PhD in Mechanical Engineering from Cranfield University. He is an Assistant Professor and currently the Dean of Mechanical Engineering Department at K.N. Toosi University of Technology. His research and teaching interests are in the field of internal combustion engines, turbomachinery and turbochargers, and thermodynamics. He has published many research papers in different journals and conference proceedings.

1 Introduction

In this work an exhaustive modelling of air intake and fuel injection systems of a turbocharged diesel engine equipped with Variable Geometry Turbine (VGT), Exhaust Gas Recirculation (EGR) and Electronic Fuel Injection (EFI) is implemented. According to the generated model a novel computer code has been developed. Then a fuzzy controller, which is a strong control approach, has been designed and used in AFR control that is of great importance in engine emission and performance. The designed fuzzy controller has a decent performance and acts reasonably fast.

The drive to reduce emissions and fuel consumption whilst meeting improved performance objectives has led to several advances in diesel engine technology in recent years. EGR, VGT and EFI systems are playing a crucial role in achieving these aims. Today's diesel engines have great flexibility to make use of advanced control systems. One important step is the control of the individual Air-to-Fuel Ratio (AFR) control which is a good representation of the power produced by engine. AFR control culminates in high combustion efficiency of the engine, frugality in fuel consumption and meeting the established emission legislations. It results from two main inputs: injection quantity and intake air mass flow quantity. For this purpose EFI system is considered as the actuator. In other words, by varying the amount of injected fuel, AFR can be controlled and maintained in an acceptable frame-work.

The introduced models for air intake system and fuel injection system are nonlinear models. Linearisation of this nonlinear engine model results in a model which is valid only in a small region around engine working point. So the use of nonlinear controllers is necessary. Fuzzy logic methodology is the applied nonlinear control method in this work.

Several design oriented and control oriented diesel engine models have been derived. Ouenou-Gamo et al. (1997) presented a theoretical model for air intake process of a turbocharged diesel engine. This model describes the dynamics of the air into the manifold and the intake phase by physical equations. Guzzella and Amstutz (1998) intended to give an overview of models and controls of diesel engines. A complete dynamic model of a diesel engine for the purpose of emission and EGR control was described in the work. Kolmanovsky et al. (1998) summarised recent developments in turbocharged diesel engine models, equipped with VGT and EGR. Fredriksson (1999) in his work deals with the problem of using the engine as an actuator to investigate the potential with integrated powertrain control through mean-value engine modelling. Silverlind (2001) studied engine modelling in Modelica which was covering the range of models known as mean-value engine models. In addition, Biteus (2002) has also implemented a mean-value engine model of a heavy duty diesel engine for the first time. Jung (2003) investigated mean-value modelling and robust control of the air path of a diesel engine equipped with VGT and EGR. The model is derived with a focus on the parameterisation of the turbocharger. It should be noted that there are lots of diesel engine models, but they are very similar to each other and they have slight differences.

Also a number of Common Rail Injection (CRI) systems have been developed and published over the last few years. Ahlin (2000) described the behaviour of pressure in common rail diesel injection system mathematically. This model was based on well known physical relations. Su et al. (2001) developed the working principle and configuration of the common rail injector through computer simulation and experimental

study. Lee et al. (2002) represented a detailed mathematical model of all diesel fuel injection system components using principles of fluid dynamics. Gullaksen (2003) developed a computer program that implemented the numerical simulation of equations for plunger, needle dynamics and transient flow in high pressure pipe-line. Kiijarvi (2003) studied the injection process of a medium-speed diesel engine using a computer program for this purpose. Seykens et al. (2004) studied the interaction between fuel properties and injection, making use of a hydraulic model of a research type heavy duty common rail fuel injection system.

Modern control systems have been applied extensively in internal combustion engines and automotive engineering control problems. Von Altrock (1994) pointed to case studies in antilock braking systems, engine control and automatic gearbox control via fuzzy logic design techniques. Thornhill and Thompson (1999) utilised an adaptive fuzzy logic control scheme to track a reference engine rotational speed during engine idling. Wijetunge et al. (2000) examined the effects of engine control strategy on emissions, fuel consumption and drivability of a high speed direct injection diesel engine equipped with VGT and EGR, utilising fuzzy logic. Howlett et al. (1999) and Hafner et al. (2000) investigated the application of fast neural net models for combustion monitoring, onboard diagnosis and enhanced control strategies as well as engine control design purposes. Diao and Passino (2001) designed a fault-tolerant control scheme for a turbine engine based on stable adaptive fuzzy/neural control, where its online learning capabilities were used to capture the unknown dynamics caused by faults. Rajagopalan et al. (2003) described the development of new control strategies such as fuzzy logic and models for hybrid electric vehicles. Hiroyasu et al. (2003) studied the recently developed HIDECS-GA computer code to optimise diesel engine emissions and fuel economy using genetic algorithms. Most recently, Tutuncu and Allahverdi (2007) described the reverse modelling of a diesel engine performance and emission characteristics by fuzzy clustering method and adaptive neural fuzzy inference system.

After all, dynamic system simulation software is an important tool for developing reliable engine control systems. Hence, all the equations and submodels of this work are simulated in Matlab/Simulink software.

2   Air intake system

One of the major factors in calculating air-to-fuel ratio of a turbocharged diesel engine is air mass flow rate. For precise calculation of this parameter a detailed, analytical and mathematical model of air intake process is required. A turbocharged diesel engine has these components in its intake system as shown in Figure 1: compressor, intercooler, EGR circuit and intake manifold.

EGR is a well-established technique for reducing in-cylinder engine NOx production. A fraction of the exhaust gas is fed into the inlet manifold to mix with the incoming fresh air. The EGR flow is controlled by a valve between intake and exhaust manifolds.

Moreover, a fixed geometry turbocharger will provide a fixed pressure ratio in a given engine speed and load, while a Variable Geometry Turbocharger (VGT) provides a range of compressor pressure ratios in any given engine condition. Adjustable nozzle vanes at the entry to the turbine alter the flow cross-sectional area into the turbine.

All the components of air intake system are modelled using physical relations such as ideal gas law, conservation of mass and energy equations and some experimental equations.

Figure 1   Schematic diagram of a turbocharged diesel engine
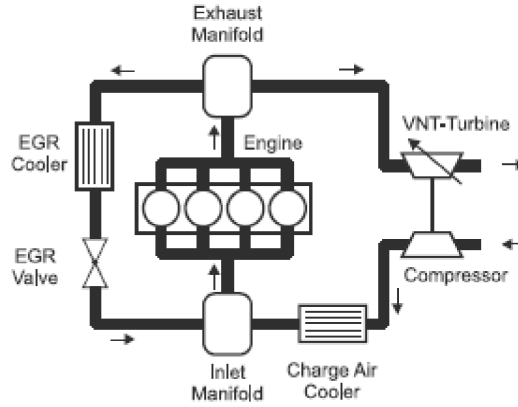
Source: Nyberg et al. (2001)

2.1   Compressor

Air characteristics after compressor, especially pressure and temperature, are fundamental elements of intake mass flow rate. Work is done on compressor from an external source by turbocharger rotating shaft. The differential equation for calculating the downstream compressor pressure is as follows:

$$\frac{dp_c}{dt} = \frac{\eta_c}{\dot{m}_c \cdot R \cdot T_{atm}} \cdot p_{atm}^{\frac{\gamma-1}{\gamma}} \cdot p_c^{\frac{1}{\gamma}} \cdot \dot{W}_c \tag{1}$$

It is assumed that the compressor efficiency is constant during the intake phase and is equal to 0.51. The definition of compressor isentropic efficiency leads to a differential equation for compressor downstream temperature:

$$\frac{dT_c}{dt} = \frac{1}{\dot{m}_c \cdot c_p} \cdot \dot{W}_c \tag{2}$$

The power is transmitted from turbine to compressor by a rotating shaft. The mathematical modelling is available in Ghazimirsaied et al. (2006). Compressor mass flow rate modelling is done based on assumptions made in Theotokatos and Kyrtatos (2001):

$$\frac{dm_c}{dt} = \frac{P_{im} - P_{atm}}{l/A} \tag{3}$$

2.2   Intercooler

The downstream temperature of intercooler is calculated using the effectiveness of heat exchanger and an appropriate coolant temperature (Jung, 2003):

$$T_{c,ic} = \eta_{he}T_{cool} + (1-\eta_{he})T_c \tag{4}$$

It is assumed that the heat exchanger efficiency is constant and is equal to 0.73. Pressure drop across the intercooler is neglected. So pressure is the same before and after this device.

2.3   Intake manifold

Making use of mass and energy balance equations for the intake manifold volume, the following differential equations are derived for pressure and mass of air inside the intake manifold:

$$\frac{dM_{im}}{dt} = \dot{m}_c + \dot{m}_{egr} - \dot{m}_{cyl} \tag{5}$$

$$M_{im}c_p\frac{dT_{im}}{dt} = -\dot{m}_c c_p T_c + \dot{m}_{egr} c_p T_{eg} + \dot{m}_{cyl} c_p T_{im} \tag{6}$$

Temperature of exhaust gases is computed from an experimental equation. Having pressure and mass of air in this region, the pressure is computed by applying the ideal gas law:

$$P_{im} = \frac{R \cdot T_{im} \cdot M_{im}}{V_{im}} \tag{7}$$

2.4   Valve section

The air intake flow depends on its density, its velocity through the valve section and cross sectional area of the input port:

$$\dot{m}_{cyl} = \rho_{csa}.u_{csa}.A_{csa} \tag{8}$$

The air density through the valve section is given by assuming isentropic condition considering an adapted neck:

$$\rho_{csa} = \frac{P_{im}}{RT_{im}}\left(\frac{P_{cyl}}{P_{im}}\right)^{\frac{1}{\gamma}} \tag{9}$$

Air velocity is computed by energy conservation equation of the air between the intake manifold and the valve section:

$$u_{csa} = \sqrt{\frac{2\gamma}{\gamma-1}\left(\left(RT_{im} - \frac{P_{cyl}}{\rho_{csa}}\right) + R(T_{im} - T_{atm})\right)} \tag{10}$$

For calculating the flow cross sectional area, the following equation is used (Heywood, 1988):

$$A_{csa} = \pi x_p \cos\beta\left(D_v - 2w + \frac{x_p}{2}\sin 2\beta\right) \tag{11}$$

If: $0 < x_p < \dfrac{w}{\sin\beta\cos\beta}$.

$$A_{csa} = \pi D_m \left[(x_p - w\tan\beta)^2 + w^2 \right]^{\frac{1}{2}}$$

(12)

If: $\dfrac{w}{\sin\beta\cos\beta} < x_p < \left[\left(\dfrac{D_p^2 - D_s^2}{4D_m} \right) - w^2 \right]^{\frac{1}{2}} + w\tan\beta$

$$A_{csa} = \frac{\pi}{4} \left(D_p^2 - D_s^2 \right)$$

(13)

If: $x_p > \left[\left(\dfrac{D_p^2 - D_s^2}{4D_m} \right) - w^2 \right]^{\frac{1}{2}} + w\tan\beta$

In the above equations: $D_m = D_v - w$. And the valve lift expression is given by (Ouenou-Gamo et al., 1997):

$$x_p = b \left(1 - \cos^2\varphi_{cs} \left(1 - \frac{b^2}{a^2} \right) \right)^{-0.5} - b$$

(14)

a and *b* are the long and the short axis of an ellipse respectively and φ_{cs} is the camshaft angular position.

2.5 EGR circuit

It is assumed that no mass is accumulated in the EGR system. So it can be modelled with static equations rather than with differential equations. The flow through the EGR valve is determined by standard orifice flow equation (Heywood, 1988):

$$\dot{m}_{egr} = \frac{A_{egr} P_{em}}{\sqrt{RT_{em}}} \sqrt{\frac{2\gamma}{\gamma - 1} \left(P_r^{\frac{2}{\gamma}} - P_r^{\frac{\gamma+1}{\gamma}} \right)}$$

(15)

With the following definition for pressure ratio:

$$P_r = \max\left(\frac{P_{im}}{P_{em}}, \left(\frac{2}{\gamma+1} \right)^{\frac{\gamma}{\gamma+1}} \right)$$

(16)

Effective area of EGR valve is computed from a second order polynomial function according to EGR valve position. EGR valve position is changing from 0 (completely closed) to 1 (completely open). EGR temperature is assumed to be constant. Its value is set to 700 K.

2.6 Cylinder dynamics

The cylinder volume during admission phase depends on the piston stroke and the cylinder section. Variations of cylinder volume are expressed by the following differential equation:

$$\frac{dV_{cyl}}{dt} = A_{cyl} r \dot{\varphi} \sin \varphi \left(1 + \frac{\cos \varphi}{\sqrt{\lambda^2 - \sin^2 \varphi}} \right) \qquad (17)$$

Furthermore, derivation form of the cylinder temperature is as follows:

$$\frac{dT_{cyl}}{dt} = \frac{1}{m_{cyl}} \left(\gamma \frac{p_{cyl}}{RP_{csa}} - T_{cyl} \right) \dot{m}_{cyl} + \frac{1}{c_v m_{cyl}} \dot{W}_{ad} \qquad (18)$$

And cylinder pressure is calculated by differentiating the ideal gas law:

$$\frac{dP_{cyl}}{dt} = \frac{1}{V_{cyl}} \left(RT_{cyl} \dot{m}_{cyl} + Rm_{cyl} \dot{T}_{cyl} - P_{cyl} \dot{V}_{cyl} \right) \qquad (19)$$

2.7 Engine block

Variation of crankshaft angular position according to time is the definition of engine speed:

$$\frac{d\phi}{dt} = N \qquad (20)$$

Engine dynamic response to variations of speed is shown by the following equation:

$$\frac{dN}{dt} = \frac{-W_{ad} - M_{load}}{J_e} \qquad (21)$$

During the air intake phase, the system composed of air at a pressure P_{cyl} in the cylinder of volume dV_{cyl} receives an energy which its expression is:

$$\frac{dW_{ad}}{dt} = -P_{cyl} \dot{V}_{cyl} \qquad (22)$$

2.8 Exhaust manifold

Exhaust manifold parameters are described by the filling and emptying model as well as by the first law of thermodynamics. Exhaust manifold temperature is coupled to EGR temperature and to the turbocharger:

$$M_{em} c_p \frac{dT_{em}}{dt} = (\dot{m}_{fuel} + \dot{m}_{cyl}) c_p T_{eg} - \dot{m}_{egr} c_p T_{em} - \dot{m}_{em} c_p T_{em} \qquad (23)$$

Air flow dynamics in exhaust manifold can be described as a first order lag:

$$\frac{dM_{em}}{dt} = \dot{m}_{fuel} + \dot{m}_{cyl} - \dot{m}_{egr} - \dot{m}_{em} \qquad (24)$$

Again the pressure of exhaust manifold is calculated from the relation of ideal gas law:

$$P_{em} = \frac{R \cdot T_{em} \cdot M_{em}}{V_{em}} \qquad (25)$$

2.9 Turbine

For obtaining mass flow circulating through the turbine and its outlet pressure experimental equations are used (Salcedo et al., 2001):

$$\dot{m}_t = A\left(1 - e^{-B\left(\frac{P_{em}}{P_t}\right)^C}\right)$$

(26)

A, B and C parameters are polynomial functions of guide vane position of turbine. Guide vane position is changing from 0 (completely closed) to 10 (completely open). Pressure of gases after turbine is also computed from an experimental relation (Salcedo et al., 2001):

$$P_t = 10^5\left(9.10^{-7}\dot{m}_t^2 + 0.0002\dot{m}_t + 0.9981\right)$$

(27)

And the definition of turbine isentropic efficiency yields the following expression for downstream temperature of turbine:

$$T_t = T_{em}\left(1 - \eta_t\left(1 - \left(\frac{P_{em}}{P_t}\right)^{\frac{1-\gamma}{\gamma}}\right)\right)$$

(28)

It is assumed that the turbine efficiency is constant during the intake phase and is equal to 0.76. The mechanical power produced by the turbine can be calculated as:

$$W_t = c_p\left(\dot{m}_c + \dot{m}_{fuel}\right)\left(T_{em} - T_t\right)$$

(29)

This power is used for calculation of compressor power.

Finally the output parameter of intake system model is air mass flow rate into the cylinder. It should be noted that turbocharger characteristic maps are not used in the modelling because of two main reasons. Firstly, these maps were not readily available and secondly we are analysing the parameters of air intake system only in the intake phase (180 degrees of crank angle) and the variations of turbocharger characteristics are not considerable in this short time.

3 Fuel injection system

In this section the description of CRI system is presented. The turning point in achieving better combustion characteristics is to provide higher injection pressures by the application of common rail injectors.

In these systems an electronic control unit calculates and sends a signal which opens and shuts a solenoid valve to obtain the required amount of fuel to be injected at the desired instant of time. Figure 2 shows a section area of a Bosch diesel injector.

In this system the injector is connected to the high pressure fuel accumulator. The fuel pressure is controlled by the pump and remains stable at a high pressure of approximately 160 MPa. In order to control the opening and closing time of needle a working chamber is presented on top of the needle. When the solenoid valve is open,

it creates a pressure drop in working chamber and this will cause a negative force which overcomes the force of needle spring and the injection initiates.

Figure 2   Diagram of a Bosch injector
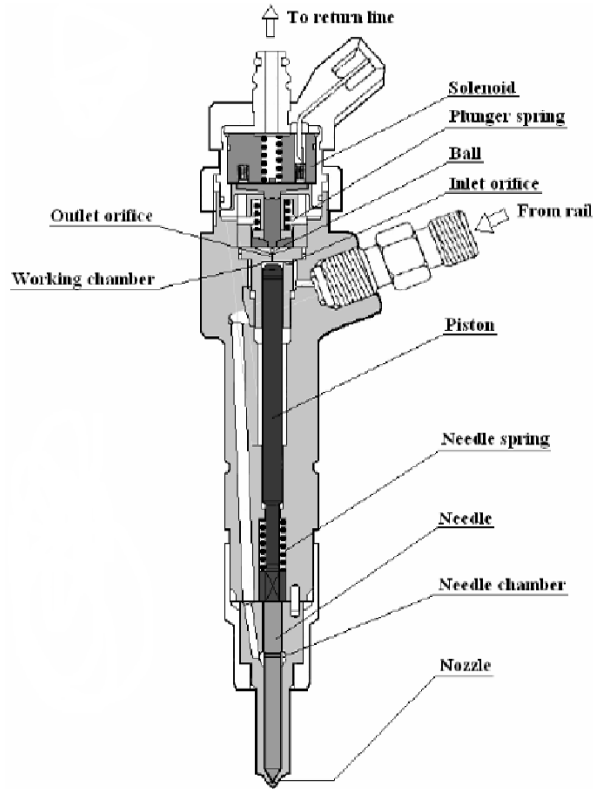
Source: Tran (2003)

3.1   Solenoid valve

It is assumed that the solenoid is extremely fast. Based on standard magnetic circuit principles (Cheung et al., 1993), the voltage equation and the consideration of back e.m.f voltage, the current of the solenoid circuit is determined from the following differential equation:

$$\frac{di}{dt} = \frac{1}{L}\left(e - R \cdot i - \frac{F(x,i)}{i} \cdot \frac{dx}{dt}\right) \tag{30}$$

And the movement of the solenoid plunger in injector is modelled by an equation from the equilibrium of forces:

$$m_1 \frac{d^2 x}{dt^2} = K_f i + P_L A_1 - m_1 g - K_1(x + x_0) - f_1 \frac{dx}{dt} \tag{31}$$

In this section it is assumed that coil inductance is constant and any possible friction due to the bulging of solenoid spring is neglected.

3.2 Hydraulic components

For modelling of hydraulic parts it is considered that pressure propagation speed is infinite. Fuel leakage between the components is ignored and pipe wall expansion is not taken into calculations. Then a one dimensional, transient and compressible flow model of CRI is built based on mass conservation and equilibrium of forces. The mass conservation relation for working chamber can be expressed as follows (Roberson and Crowe, 1997):

$$A_2 \frac{dz}{dt} - \frac{V_{wc}}{\mu} \frac{dP_W}{dt} = K_1 A_1 \sqrt{\frac{2(P_L - P_W)}{\rho}} - K_0 A_0 \frac{x}{X_{max}} \sqrt{\frac{2(P_W - P_R)}{\rho}} \tag{32}$$

By applying the Newton's second law to the injector piston, the piston system motion equation will be:

$$m_2 \frac{d^2 z}{dt^2} = P_L A_N - P_W A_2 - K_2 (y + y_0) - m_2 g - f_2 \frac{dz}{dt} \tag{33}$$

The theory of "flow through an orifice" leads to the next equation for injection flow rat (Lee et al., 2002):

$$q_I = K_I A_I \frac{z}{Z_{max}} \sqrt{\frac{2(P_L - P_W)}{\rho}} \tag{34}$$

Lastly, the injection quantity is the integral of the injection flow rate in every shot:

$$Q = \int_0^t q_I dt \tag{35}$$

In the above-mentioned equations, fuel bulk modulus and fuel density are dependent only on fuel pressure. They are also dependent on temperature but in a smaller scale. Polynomial equations are used to define these dependencies. Fuel bulk modulus is depending on pressure based on the following equation (dimension of P is Pascal) (Boehman et al., 2003):

$$\mu = 5P + 1361714.565 \tag{36}$$

And fuel density is calculated by the following second order polynomial (Kiijarvi, 2003):

$$\rho = -1.3846 \cdot 10^{-15} P^2 + 5.8738 \cdot 10^{-7} P + 818.67 \tag{37}$$

The output of this model is fuel injection quantity which is necessary for calculating and control of air-to-fuel ratio.

4 AFR control

Air mass flow rate into cylinders and fuel injection quantity are complex nonlinear functions of several interactive variables, which together present a highly coupled plant. Air-to-fuel ratio of an engine can be controlled by three different controllers. Two of these controllers are located in air intake system and the third one is located in injection system. EGR and VGT valves as controllers play a significant role in emissions, fuel consumption and drivability of a vehicle. The settings of VGT vane and EGR valve alter

the engine pumping work and cylinder charge composition, affecting fuel consumption and emissions (Wijetunge et al., 2000). By changing the positions of EGR and VGT, air flow rate into cylinders will be changed. So these two controllers can be used for AFR control.

Electronic controls, which allow greater flexibility in the setting of individual parameters, make EFI an appropriate system for precise control of injection quantity and timing. By application of the ECU, the injection is no longer dependent on the position of crankshaft. High speed solenoid valves have the capability to adjust the amount of injected fuel and therefore air-to-fuel ratio. The high fuel pressure is supplied by a pump while an ECU calculates and sends a signal (voltage of solenoid circuit) to injector which opens and shuts a solenoid (Tran, 2003). Consequently this kind of fuel injection system can be used for control of AFR.

In this work the positions of EGR and VGT valves are set manually for different engine speeds. However the controller for AFR control is solenoid valve and fuel injection system. In other words, the fuzzy controller calculates a new value for the bandwidth of solenoid voltage signal. This value works as a new input for the fuel injection subsystem. Modified amount of fuel injection quantity is obtained making use of this new bandwidth value.

In order to eliminate the steady state error of the system a fuzzy integrator is used. The equation for this integrator is presented as follows:

$$BW_{new} = BW_{old} - C\left(AFR_{ref} - AFR_{est}\right) \tag{38}$$

In this relation, C is the fuzzy controller output; AFR_{ref} is the desired AFR and AFR_{est} is the calculated air-to-fuel ratio. BW is representing the value of solenoid voltage bandwidth (the control signal). The general structure of the control system is shown in Figure 3.

Figure 3   Schematic diagram of the control system
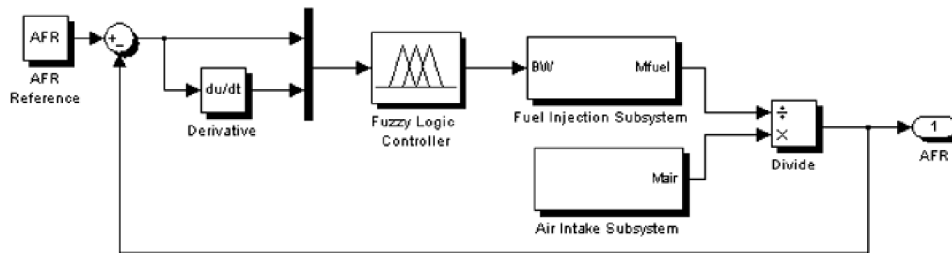

4.1   Control strategy

A complete description of the methodology of fuzzy logic is beyond the scope of this paper, however the interested reader is referred to Pedrycz (1989) and Wang (1996) for a deeper insight. The controller used in this work was designed using the Matlab fuzzy logic toolbox, employing a graphical interface to simplify the task.

The first stage of the fuzzy controller design is to decide on a structure. From the analysis of the problem it is clear that the inputs to the system need to be AFR error (difference between desired and actual AFR) signal and the derivation of the AFR error signal. Knowing AFR error and the AFR error derivation signals, one can decide for a

new bandwidth value. The output of the controller is the *C* factor in the equation of fuzzy logic integrator.

The next step is defining membership functions for inputs and outputs. They are illustrated in Figure 4. The shape of a membership function can be an arbitrary curve whose shape we can define as a function that suits us from the point of view of simplicity, convenience, speed, stability and efficiency. One usually can get along well with just one or two types of membership functions, for example, triangle or trapezoid functions. Selection of the numbers of membership functions is optional. Usually odd numbers of membership functions, 3, 5, 7, 9 or more, are chosen. Typically, most papers and documents select seven membership functions. Selecting more than seven membership functions increases the number of rules. Besides, using more membership functions does not necessarily improve the performance of the controller and its effect is usually trivial. Inputs and outputs are covered by seven triangular membership functions. The first input (AFR error) is varying from –1 to +1. The second input is also varying from –1 to +1. The output is varying from –1 to +1 too (Shamekhi, 2004). It should be noted that we have used a normalised database. Two gains are applied to alter the real variation bounds of AFR error and its derivation to normalised range which is between –1 and +1.

Figure 4   Normalised data base
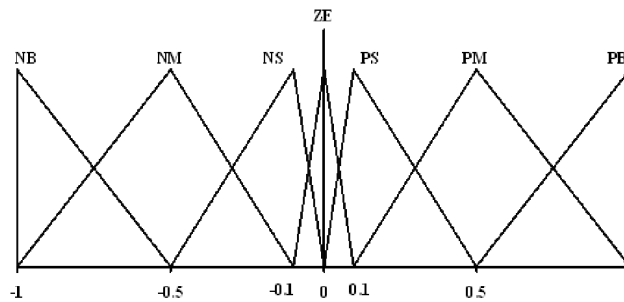
The final step is to define the rules for the controller. They are simply an embodiment of the control action one wishes to be achieved. For this work 49 rules are defined. When the error is negative it shows that the actual AFR is greater than the desired AFR. It means that injected fuel quantity is small. So injection quantity should be increased in order to reduce the AFR magnitude. Consequently, control signal bandwidth needs to be increased. On the contrary, when the error is positive it indicates that actual AFR is smaller than desired AFR. And it tells us that injected fuel quantity is high and it should be decreased in order to raise the AFR magnitude. Therefore, control signal bandwidth needs to be decreased. These statements are the fundamentals of defining the base rule. Based on the defined membership functions for inputs and output and the notation which is used according to Figure 4, the following rules are derived for the purpose of AFR control. The rules that are used are expressed in Table 1.

An if-then fuzzy rule like "IF <FP1> THEN <FP2>", will be interpreted in Mamdani implication with the following membership functions:

$$\mu_{Q_{MM}}(x, y) = \min\left(\mu_{FP1}(x), \mu_{FP2}(y)\right) \quad or \quad \mu_{Q_{MM}}(x, y) = \mu_{FP1}(x) \times \mu_{FP2}(y) \qquad (39)$$

Algebraic product is used in the implementation of Mamdani implication in this work.

Table 1   Rule base used for the purpose of AFR control

$\dot{e}$ \ e	NB	NM	NS	ZE	PS	PM	PB
NB	PB	PB	PB	PB	PM	PM	PS
NM	PB	PM	PM	PM	PS	PS	ZE
NS	PM	PM	PS	PS	PS	ZE	ZE
ZE	PS	PS	PS	ZE	NS	NS	NM
PS	ZE	ZE	NS	NS	NM	NM	NM
PM	ZE	NS	NM	NM	NM	NB	NB
PB	NM	NB	NB	NB	NB	NB	NB

Assume that $Ru^{(l)}$ is a fuzzy relation and shows a fuzzy if-then rule. Using $\dot{+}$ symbol for S-norm, then the combination of rules in fuzzy rule base, according to Mamdani inference rule, will be defined as follows (Wang, 1996):

$$\mu_{Q_M}(x,y) = \mu_{Ru^{(1)}}(x,y) \dot{+} \cdots \dot{+} \mu_{Ru^{(M)}}(x,y) \tag{40}$$

Algebraic sum is the method which is employed for implementation of S-norm (aggregation) with the following definition:

$$S_{as}(a,b) = a + b - ab \tag{41}$$

For 'fuzzy and' method fuzzy intersection with definition of minimum class is used. *A* and *B* are two fuzzy sets:

$$\mu_{A \cap B}(x) = \min(\mu_A(x), \mu_B(x)) \tag{42}$$

For 'defuzzification' method centroid of area defuzzifier (centroid) method has been chosen:

$$y^* = \frac{\int_V y\mu_{B'}(y)dy}{\int_V \mu_{B'}(y)dy} \tag{43}$$

Centre of gravity defuzzifier has two main advantages comparing with other methods of defuzzification: justifiability and continuity.

5   Model validation

Output of the air intake model is measured for different engine speeds and the results of this model are compared with available experimental data (Jung, 2003). The comparison between simulated and experimental data is shown in Figure 5.

Measurements have also performed for various solenoid control pulses with durations of 4, 6, 8 and 10 ms. The results of measurements together with experimental data (Tran, 2003), are shown in Table 2. These figures show a very good match between the experimental and simulated results.

Figure 5 Validation diagram for air intake system
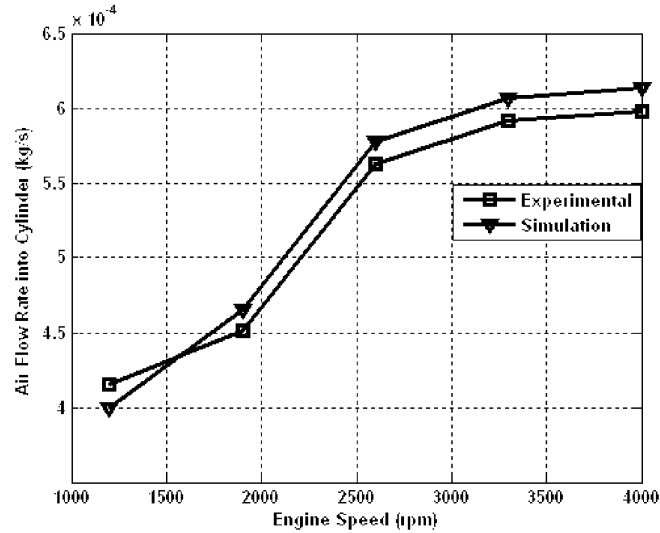
Table 2 Comparison of simulated and experimental injection quantities per injection

Duration of pulses (ms)	Measured quantity of injection (mg)	Simulated quantity of injection (mg)	Error (%)
4	114	115.89	1.6
6	172	169.017	−1.7
8	227	22.402	−2
10	284	275.825	−2.8

It should be noted that the magnitude of voltage during injection is assumed to be constant (15 V). Generally speaking, there is a good consistency between simulation results and experimental data.

6 Simulation results

All the above-mentioned nonlinear and coupled differential and ordinary equations are coded in Matlab/Simulink software. The basic engine parameters are listed in Table 3.

Table 3 Basic engine parameters

|	
Cylinder bore	0.0725 (m)
Compression ratio	17 : 1
Crank radius	0.05 (m)
Connecting rod length	0.12 (m)
Displacement volume	4.2×0^{-4} (m^3)
Piston stroke	0.1 (m)

Engine speed in the following diagrams is 1200 rpm. The values of turbine valve position and EGR valve position are set to 1 and 0.35 respectively. It should be noted that EGR and VGT valve positions are altered appropriately in assorted engine speeds. It is also assumed that intake process starts precisely from TDC and ends exactly at BDC. So the duration of intake phase is 180 crank angle degrees.

Intake manifold pressure and temperature diagrams are shown in Figures 6 and 7. According to these graphs, both temperature and pressure have increased. This rise is because of augmentation of a portion of exhaust gases through EGR system into intake manifold. These figures show 13 degrees increase in temperature and 10 kPa increase in pressure during the intake phase in intake manifold.

**Figure 6**   Intake manifold pressure (simulation)
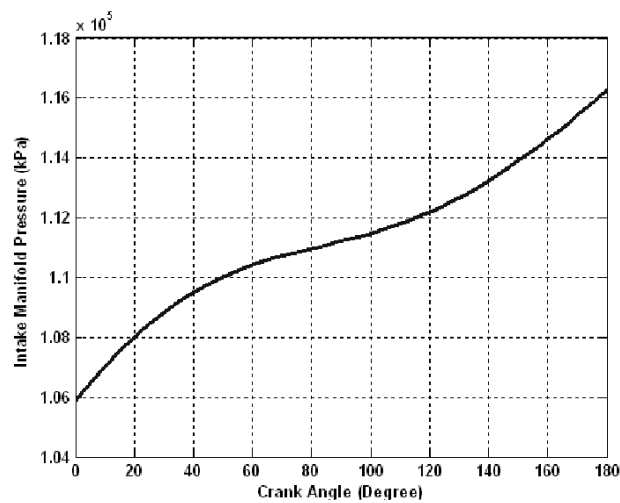
Figure 7   Intake manifold temperature (simulation)
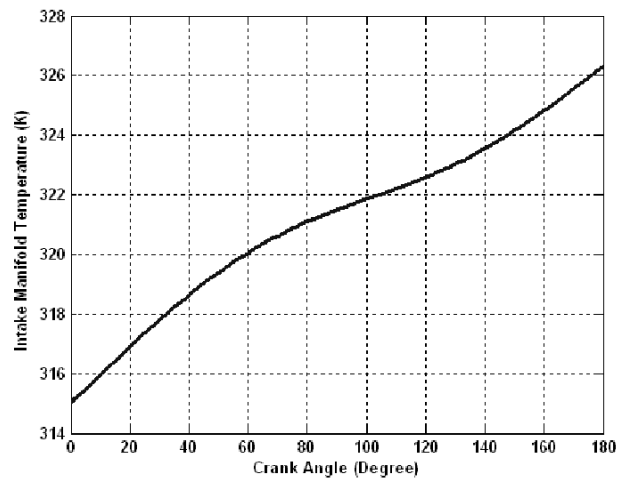
Mass of air entering the cylinder is one of the two main parameters which are needed for computing and controlling the AFR. Figures 8 and 9 show the profile of cylinder air mass flow rate and cylinder charge during the intake phase.

Figure 8   Air flow rate into cylinder (simulation)
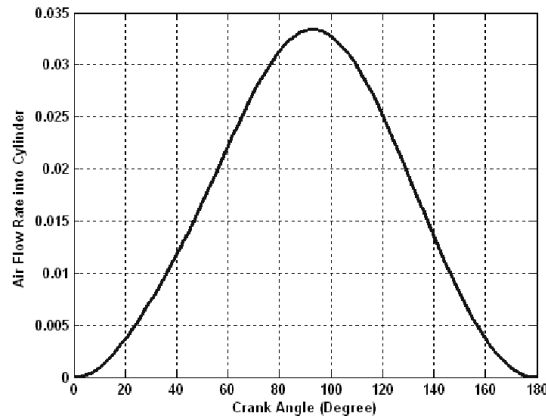
Figure 9   Mass of air in the cylinder (simulation)
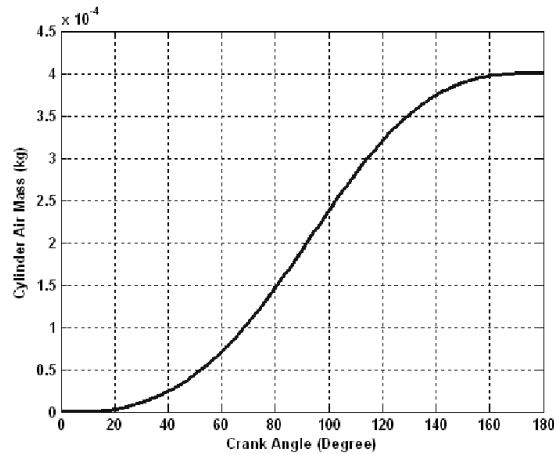

Figure 8 shows the standard profile for opening and closing the air intake valve. Increase in valve lift results in increase in air flow rate into cylinder. When the valve reaches its maximum lift, air flow rate has its greatest magnitude. It is assumed that intake valve opens exactly at the beginning of intake process and closes exactly at the end of intake phase. Integrating from air flow rate into cylinder we can calculate the amount of air entered the cylinder up to every time instant.

At the end of exhaust phase in previous engine cycle, the temperature of exhaust gases was high (around 700 K). As the air intake valve opens, fresh air enters the cylinder and temperature decreases. At the end of intake phase the temperature in the cylinder reaches the value of 315 K (near to intake manifold temperature). Cylinder temperature variation is shown in Figure 10.

**Figure 10** Cylinder temperature variations (simulation)
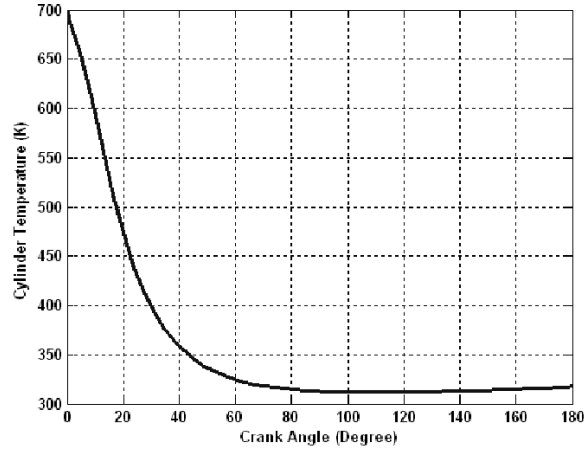
According to Figure 11, cylinder pressure increases nominally at the beginning of intake phase. It has two main reasons: firstly, intake manifold pressure is high and secondly, air intake valve is closed at the very beginning of intake process. Then because of accelerating downward movement of piston and more opening of intake valve, pressure declines and again by entering more air into cylinder and by completing the filling process cylinder pressure rises and approaches the intake manifold pressure at the end of intake phase.

**Figure 11** Cylinder pressure variations (simulation)
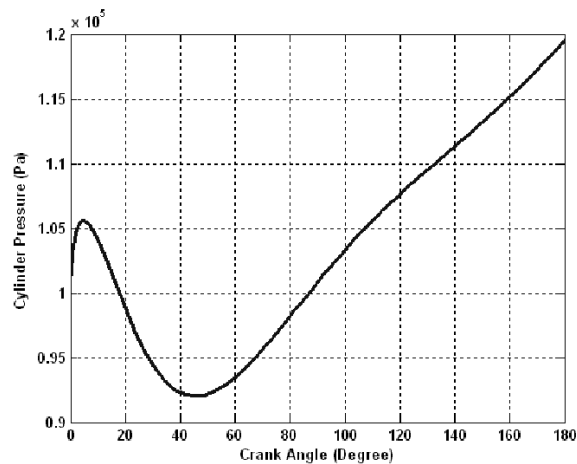
A control pulse of 15 V DC with the duration of 5 ms is applied to solenoid circuit in order to obtain the quantity of injection. In computing the quantity of injected fuel, the time of injection is not important. So the simulation results are shown vs. a sample time rather than crank angle. 5 ms duration of injection mean that injection is occurred in 36 degrees of crank angle, no matter when it happens. The shape of this signal is seen in Figure 12.

The shape of needle movement is also illustrated in Figure 12. Solenoid plunger movement and needle movement both comply with the shape of applied voltage to the solenoid circuit. According to Figure 13, needle movement and applied voltage are not simultaneous and the needle moves with a short delay in comparison with voltage signal.

**Figure 12** Control signal (voltage) of solenoid (simulation)
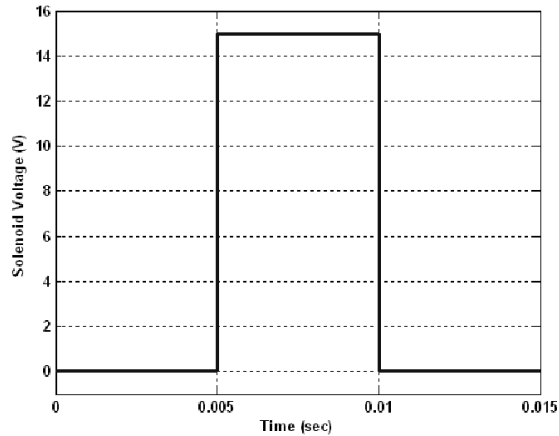
Figure 13 Needle movement (simulation)
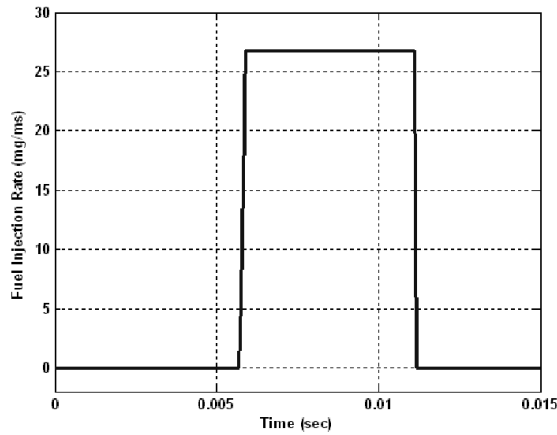
The profile of injection rate of a six nozzle injector during injection phase is shown in Figure 14. The shape of injection rate follows the shape of needle movement. As the needle lifts from its seat injection initiates and injection rate rises as the needle lifts more. When the needle moves back to its first position injection ceases.

By integrating the injection rate in one injection duration we can obtain the quantity of injection in each time during injection period. The shape of injection quantity is shown in Figure 15.

Figure 14 Rate of injection (simulation)
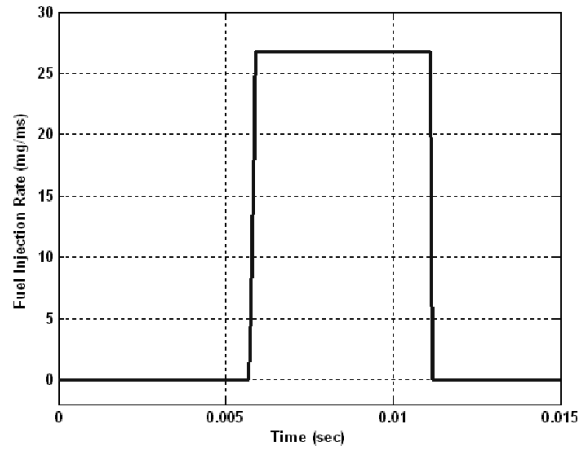
Figure 15 Injection quantity in one injection duration (simulation)
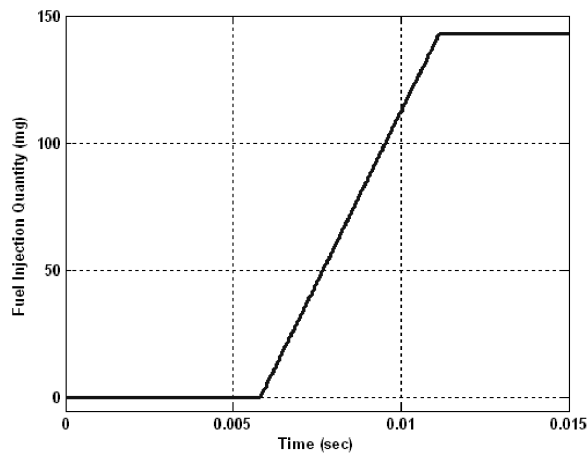
We were also interested in investigation of the sensitivity of major output parameters of the injector: injection delay, injection quantity and injection duration. The results of sensitivity analysis showed that the system is relatively insensitive to changes in force coefficients of solenoid and needle springs, but it is very sensitive to the solenoid temperature (Shamdani et al., 2006). The results are shown in Table 4:

Table 4   Sensitivity analysis of CRI Model

	k_1	k_2	d_p	T_s
Injection delay	−0.173	0.085	0.69	1.6
Injection duration	−0.049	−0.051	−0.05	−0.512
Injection quantity	−0.061	−0.059	−0.068	−0.638
Injection delay	−0.173	0.085	0.69	1.6

Figure 16 illustrates the behaviour of designed fuzzy logic controller. Fuzzy logic controller reaches the desired value of AFR (in this case 45) in about 0.8 seconds. This figure shows the performance of controller when the engine speed is 1200 rpm. So this controller is capable to adjust the AFR in less than 8 complete thermodynamic engine cycles (each engine thermodynamic cycle at 1200 rpm speed is 0.1 seconds). The type of membership functions and governing rules in the rule base as well as the fuzzifiers are selected in such a way that guarantees the stability of the system and controller. According to the propositions numbered 17-1 to 17-3 in 17th chapter of Wang (1996), the stability of the controller is warranted by selection of the specified membership functions, fuzzy rules and fuzzifiers. It should be mentioned that we have chosen the same membership functions, fuzzy rules and fuzzifiers.

Figure 17 shows the variation of error signal. At first the error is about 10 and gradually after 0.8 seconds error declines to zero. It means that the controller has reached the value of AFR to desired value exactly. The value of AFR was at first 30. We assumed that the desired value of AFR is 45.

Figure 16 Behaviour of fuzzy logic controller (simulation)
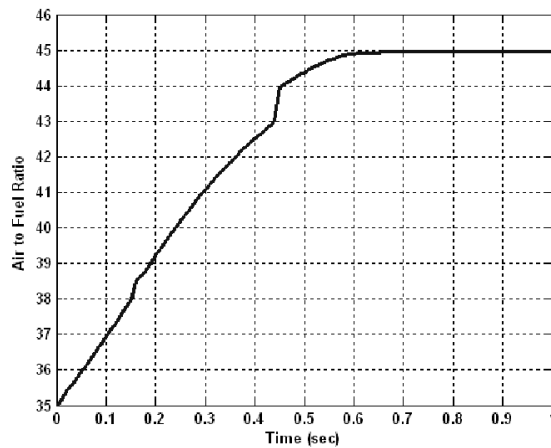
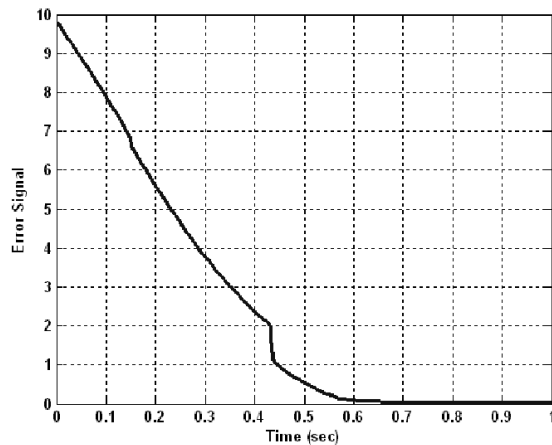**Figure 17** Variation of error signal magnitude (simulation)

Figure 18 represents the profile of control signal variations. The actual AFR is less than the desired AFR. So the AFR should be increased. Decreasing the value of solenoid voltage bandwidth reduces the amount of injected fuel and this will culminate in raised AFR. As seen in Figure 18 the signal bandwidth has fallen from 0.00343 seconds to 0.00257 seconds during a 0.8 second period.

The controller performance as it is observed in Figures 16–18 is quite fast and it reaches a plateau at the end when the AFR is equal to the desired value.

Figure 18 Variation of solenoid voltage signal bandwidth (simulation)
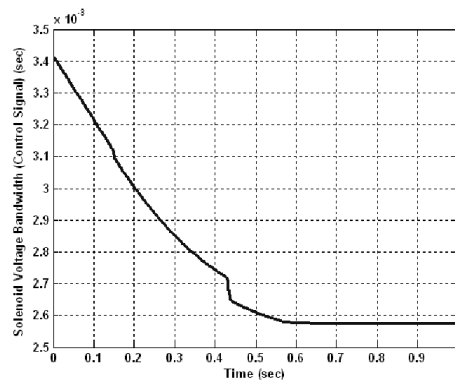
7   Conclusion

In this work, a detailed theoretical model for air intake system and EFI system of a turbocharged diesel engine based on physical relations is proposed. These mathematical models are programmed in Matlab/Simulink software environment. The objective has been to calculate the amount of air entering the cylinder during intake process and injected fuel quantity during one injection period. A fuzzy controller based on fuzzy logic methodology is designed for the purpose of air-to-fuel ratio control of the engine.

Finally, the main conclusions are as follows:

- A comprehensive model of air intake and injection systems of turbocharged diesel engines equipped with EGR and VGT has been developed.

- A new computer code, based on the developed model, has been generated.

- The simulation results for air intake model agree reasonably well with available experimental data.

- There is a good consistency between simulated and measured data for EFI system.

- Air-to-fuel ratio control is performed make use of a fuzzy control theory, which is a powerful control methodology, with 49 rules.

- Fuzzy controller performance is quite fast. It corrects the value of AFR and adjusts its quantity to the desired value in fewer than eight complete engine cycles by varying the fuel injected quantity through changing the magnitude of solenoid voltage signal bandwidth.

References

Ahlin, K. (2000) *Modeling of Pressure Waves in the Common Rail Diesel Injection System*, MSc Thesis, Department of Electrical Engineering, University of Linkoping, Sweden.

Biteus, J. (2002) *Mean Value Engine Model of a Heavy Duty Diesel Engine*, MSc Thesis, Department of Electrical Engineering, Linkopings University, Sweden.

Boehman, A., Alam, M., Song, J., Acharya, R., Szybist, J. and Zello, V. (2003) 'Fuel formulation effects on diesel fuel injection, combustion, emissions and emission control', *Diesel Engines Emissions Reduction Conference*, Pennsylvania State University, USA.

Cheung, N.C., Rahman, M.F. and Lim, K.W. (1993) 'Simulation and experimental studies towards the development of a proportional solenoid', *Australian Universities Power Engineering Conference*, Australia.

Diao, Y. and Passino, K.M. (2001) 'Stable fault-tolerant adaptive fuzzy/neural control for a turbine engine', *IEEE Transactions on Control Systems Technology*, Vol. 9, No. 3, pp.494–509.

Fredriksson, J. (1999) *Nonlinear Control of Turbocharged Diesel Engines*, Licentiate's Thesis, Departments of Signals and Systems, Chalmers University of Technology, Sweden.

Gullaksen, J. (2003) *Simulation of Diesel Fuel Injection Dynamics*, MSc Thesis, Department of Mechanical Engineering, Technical University of Denmark, Denmark.

Guzzella, L. and Amstutz, A. (1998) *Control of Diesel Engines*, 0272-1708/98, IEEE.

Hafner, M., Schuler, M., Nelles, N. and Isermann, R. (2000) 'Fast neural networks for diesel engine control and design', *Control Engineering Practice*, Vol. 8. pp.1211–1221.

Heywood, J.B. (1988) *Internal Combustion Engine Fundamentals*, McGraw-Hill Book Company, New York, USA.

Hiroyasu, H., Miao, H., Hiroyasu, T., Miki, M., Kamiura, J. and Watanabe, S. (2003) *Genetic Algorithms Optimization of Diesel Engine Emissions and Fuel Efficiency with Air Swirl, EGR, Injection timing and Multiple Injections*, JSAE, 20030248.

Howlett, R.J., de Zoysa, M.M., Walters, S.D. and Howson, P.A. (1999) 'Neural network techniques for monitoring and control of internal combustion engines', *International Symposium on Intelligent Industrial Automation*, Genova, Italy.

Jung, M. (2003) *Mean-Value Modeling and Robust Control of the Air Path of a Turbocharged Diesel Engine*, PhD Thesis, Hopkinson Lab, Department of Engineering, University of Cambridge, UK.

Kiijarvi, J. (2003) *Diesel Fuel Injection System simulation*, Doctor of Technology Thesis, Publications of the Internal Combustion Engines Laboratory, Helsinki University of Technology, Finland.

Kolmanovsky, I., Moraal, P., Niuwestadt, M. and Stefanopoulou, A.G. (1998) *Issues in Modeling and Control of Intake Flow in Variable Geometry Turbocharged Engines*, Scientific Research Laboratory, Ford Motor Company, USA.

Lee, H.K., Russell, M.F. and Bae, C.B. (2002) 'Mathematical model of diesel fuel injection equipment incorporating non-linear fuel injection', *Proceedings of the IMechE Part D Journal of Automobile Engineering*, Vol. 216, No. 3, pp.191–204.

Nyberg, M., Stutte, T. and Wilhelmi, V. (2001) *Model Based Diagnosis of the Air Path of an Automotive Diesel Engine*, DaimlerCrysler AG, Research and Technology (FT2/EA), Stuttgart, Germany.

Ouenou-Gamo, S., Ouladsine, M. and Rachid, A. (1997) *Air Intake Theoretical Model and Simulation of a Turbocharger Diesel Engine*, 0-8186-7873-9/97, IEEE.

Pedrycz, W. (1989) *Fuzzy Control and Fuzzy systems*, Research Studies Press Ltd., USA.

Rajagopalan, A., Washington, G., Rizzoni, G. and Guezennec, Y. (2003) *Development of Fuzzy Logic and Neural Network Control and Advanced Emissions Modeling for Parallel Hybrid Vehicles*, Center for Automotive Research, Intelligent Structures and Systems Laboratory, Ohio State University, USA.

Roberson, J. and Crowe, C. (1997) *Engineering Fluid Mechanics*, 6th ed., John Wiley & Sons Publications, New York, USA.

Salcedo, J.V., Pieroni, E., Perez, E., Blasco, X., Martinez, M. and Garcia, J.V. (2001) *Real-Time Control and Simulation of a Non-linear Model of Air Management in a Turbocharged Diesel Engine*, Department of System Engineering and Control, Universidad Politecnica de Valencia, Spain.

Seykens, X.L.J., Somers, L.M.T. and Baert, R.S.G. (2004) 'Modeling of common rail injection system and influence of fluid properties on injection process', *Proceedings of International Conference on Vehicle Alternative Fuel Systems and Environmental Protection*, Dublin, Ireland.

Ghazimirsaied, S.A., Shamdani, A.H. and Shamekhi, A.H. (2006) 'On the use of VVT strategy for the maximum volumetric efficiency in turbocharged diesel engines', *Internal Combustion Engine Division of ASME 2006 Spring Technical Conference*, Aachen, Germany.

Shamdani, A.H., Shamekhi, A.H., Ziabasharhagh, M. and Aghanajafi, C. (2006) 'Modeling and simulation of a diesel engine common rail injector in Matlab/Simulink', *14th Annual International Conference of Mechanical Engineering*, Isfahan, Iran.

Shamekhi, A.H. (2004) *Simulation and Fuzzy Spark Advance Control in SI engines by Ion Current Sensing*, PhD Thesis, Department of Mechanical Engineering, K.N. Toosi University of Technology, Iran.

Silverlind, D. (2001) *Mean Value Engine Modeling with Modelica*, MSc Thesis, Department of Electrical Engineering, Linkopings University, Sweden.

Su, W., Wang, Y., Xie, H. and Li, S. (2001) *A Study of Effects of Design Parameters on Transient Response and Injection Rate Shaping for a Common Rail Injector System*, State Key Labs of Engines, Tianjin University, China.

Theotokatos, G. and Kyrtatos, N.P. (2001) *Diesel Engine Transient Operation with Turbocharger Compressor Surging*, SAE Technical Conference, 2001-01-1241.

Thornhill, M. and Thompson, S. (1999) 'Adaptive fuzzy logic control of engine idle speed', *Proceedings of the I MECH E Part I Journal of Systems and Control Engineering*, Vol. 213, No. 2, pp.145–155.

Tran, X.T. (2003) *Modeling and Simulation of Electronically Controlled Diesel Injectors*, MSc Thesis, School of Mechanical and Manufacturing Engineering, the University of New South Wales, Sydney, Australia.

Tutuncu, K. and Allahverdi, N. (2007) 'Reverse modeling of a diesel engine performance by FCM and ANFIS', *Proceedings of the 2007 International Conference on Computer Systems and Technologies*, Bulgaria, Vol. 285, pp.1–7.

Von Altrock, C. (1994) 'Fuzzy logic technologies in automotive engineering', *IEEE Conference Proceedings*, pp.110–117.

Wang, L. (1996) *A Course in Fuzzy Systems and Control*. Prentice Hall Publications, New Jersey, USA.

Wijetunge, R.S., Brace, C.J., Hawley, J.G. and Vaughan, N.D. (2000) *Fuzzy Logic Control of Diesel Engine Turbocharging and Exhaust Gas Recirculation*, University of Bath, UK.

Nomenclature

A	Cross sectional area (m^2)
C_P	Specific heat at constant pressure (kJ/kgK)
D	Diameter (m)
e	Voltage (Volt)
f	Friction coefficient

F	Force (N)
g	Gravity acceleration (m/sec^2)
i	Electrical current (Ampere)
J	Inertia (kg.m^2)
k	Spring coefficient (N/m)
K	Flow coefficient
l	Length (m)
L	Solenoid inductance (H)
m	Mass (kg)
M	Torque (N.m)
N	Engine speed (rpm)
P	Pressure (kPa)
q	Injection flow rate (mg/msec)
Q	Injected fuel quantity (mg)
r	Crank radius (m)
R	Gas constant (kJ/kgK)
Rs	Resistance (Ohm)
t	Time (sec)
T	Temperature (K)
u	Velocity (m/s)
V	Volume (m^3)
w	Valve seat width (m)
W	Power, Work (kJ)
x	Solenoid plunger movement (m)
y	Piston Movement (m)
z	Needle movement (m)
Greek symbols	
β	Seat angle (degree)
Φ	Crankshaft angular position (degree)
γ	Specific heat ratio
η	Efficiency
λ	Ratio of connecting rod length to crank radius
μ	Bulk modulus (kPa)
ρ	Density (kg/m^3)
Subscripts	
0	Outlet orifice
1	Inlet orifice
2	Injector needle
ad	Admission
atm	Atmospheric conditions

c	Compressor
cool	Coolant
csa	Valve section
cyl	Cylinder
e	Engine
eg	Exhaust gases
egr	Exhaust Gas Recirculation
em	Exhaust manifold
est	Estimated
f	Force
he	Heat exchanger
im	Intake manifold
L	Fuel line
P	Valve input port
R	Fuel return line
ref	Reference
s	Valve stem
t	Turbine
v	Valve head
W	Working chamber